Preprint of: Bonanni, A. and del Valle, M. “Use of nanomaterials for impedimetric DNA sensors : a review” in Analytica chimica acta, vol. 678, issue 1 (Sep. 2010), p. 7-17. The final version is available at DOI 10.1016/j.aca.2010.08.022

Use of nanomaterials for impedimetric DNA sensors

A.Bonanni[1,2] M. del Valle[1]

[1] Sensors and Biosensors Group, Chemistry Department, Universitat Autònoma de Barcelona, 08193 Bellaterra, Barcelona, SPAIN

[2] International Center for Materials Nanoarchitectonics (MANA) / Biomaterials Center, National Institute for Material Science (NIMS), 1-1 Namiki, Tsukuba (Ibaraki), Japan

Abstract

This review presents the state of the art of DNA sensors (or genosensors) that utilize the electrochemical impedance spectroscopy as the transduction technique. As issue of current interest it is centered on the use of nanomaterials to develop or to improve performance of these specific biosensors. It will describe the different principles that may be employed in the measuring step and the different formats adopted for detection of a DNA sequence or confirmation or amplification of the finally obtained signal. The use of nanomaterials for the above listed aspects, viz. the use of carbon nanotubes or other nanoscopic elements in the construction of the electrodes, or the use of nanoparticles, mainly gold or quantum dots, for signal enhancement will be fully revised.

Keywords

Biosensor, genosensor, carbon nanotube, gold nanoparticles, quantum dots, electrochemical impedance spectroscopy

1. Introduction

Genosensors are biosensors in which the biorecognition element consists of a DNA sequence [1]. These devices combine the receptor which imparts selectivity and a transducer which provides sensitivity and converts the biorecognition event into a usable signal, in our case belonging to electric domain. The determination of nucleic acid sequences from humans, animals, bacteria and viruses is the departure point to solve different problems: investigation about food and water contamination caused by microorganisms, detection of genetic disorders, tissue matching, forensic applications etc [2-4].

Among DNA sensors, two main groups can be distinguished, according to the different protocols based on labeling DNA target or using a label-free approach. Regarding the first approach, common label used for hybridization detection can be fluorescent dyes [5, 6], redox active enzymes [7, 8] magnetic particles [9] or different kinds of nanoparticles [10, 11]. An indirect labelling scheme consist of the use of redox couple which intercalate into DNA double helix, such as metal complexes [12, 13] or organic dyes [14, 15], or the use of redox indicators in solution which improve impedance performance [16]. In a label-free approach, DNA sensors are based on the detection of unlabelled DNA sequences. This can be performed by measuring the signal due to the direct oxidation of DNA bases [17, 18] or using techniques sensitive to changes in the electrical properties of bio-modified electrode surface, such as Quartz Crystal Microbalance (QMC) [19, 20], Surface Plasmon Resonance (SPR) [21, 22] or Electrochemical Impedance Spectroscopy [16, 23].

1.1 Theoretical background

The term *impedance* was coined in 1886 by the electrical engineer, mathematician, and physicist Oliver Heaviside, who adapted complex numbers to the study of electrical circuits [24].

The method of impedance measurements is widely used in many fields of electrochemistry, e.g. electrode kinetics, double-layer studies, batteries, corrosion, solid-state electrochemistry, bioelectrochemistry.

Electrochemical Impedance Spectroscopy (EIS) is a characterization technique which provides electric information in the frequency domain [25, 26]. With this technique, a process occurring in an electrochemical cell can be modelled using combination of resistors and capacitors, i.e., a RC circuit can be built that gives the same current response that is produced by the electrochemical system. This is the principle of equivalent circuits [27]. By the use of equivalent circuits the experimental spectrum can be fitted with the theoretical curve corresponding to the selected circuit model, thus obtaining the values of electrical parameters.

Electrochemical impedance is generally measured by applying an AC potential to an

electrochemical cell and measuring the current that crosses through it. The applied sinusoidal excitation potential E_t corresponds to:

$$E_t = E_0 \cdot Sin(\omega \cdot t) \quad \textbf{(1)}$$

(where E_t is the potential at time t, E_0 is the amplitude of the signal, and $\omega = 2\pi f$ is the radial frequency; f is the frequency expressed in Hertz (Hz)).

The response to this potential is an AC current signal with a current intensity I_t also depending on t, with the same frequency but with an amplitude I_0 and a phase angle ϕ depending on the impedance of the system (as represented in Figure 1).

$$I_t = I_0 \cdot Sin(\omega \cdot t + \phi) \quad \textbf{(2)}$$

In analogy to Ohm's law the impedance of the system is:

$$Z = \frac{E_t}{I_t} = \frac{E_0 \cdot Sin(\omega \cdot t)}{I_0 \cdot Sin(\omega \cdot t + \phi)} = Z_0 \cdot \frac{Sin(\omega \cdot t)}{Sin(\omega \cdot t + \phi)} \quad \textbf{(3)}$$

In this equation we can see that the impedance is expressed in terms of a magnitude Z_0, and a phase shift ϕ. This enables to treat impedance like a vector with magnitude Z_0, and a direction given by the phase angle ϕ.

To obtain an impedimetric spectrum a small AC excitation signal (typically 5-10 mV) is applied to the system within a certain frequency range, thus obtaining an AC current response for each analysed frequency value.

For the mathematical treatment of data, a common way to represent the impedance vector model is to use complex notation, the in-phase and out-of-phase axes being the real and imaginary axes respectively. In this way all components that generate a phase shift (i.e. the capacitor) will contribute to the imaginary part of the impedance, whilst the ones that do not produce any phase shift (i.e. the resistance) will contribute to the real part.

$$Z = Z_r + jZ_i \quad (4)$$

In this way, the in-phase (Z_r) component is due to any resistive component in the system, while the out-phase (Z_i) is more related to the formation of insulating layers (viz. the electrochemical double layer, or any added barrier).

Among the different graphical representations of impedimetric data, the most common is

represented by the 'Nyquist plot', in which the imaginary part of the impedance Z_i is plotted versus the real part Z_r. In this plot each point corresponds to a different frequency. The low frequency data are represented on the right part of the diagram whilst the high frequency data are on the left one.

The interpretation of impedimetric spectra is based on the correlation among the obtained data with equivalent circuits formed by basic electrical elements such as resistance, capacitance, and inductance combined among them, thus generating comparable impedimetric spectra provided by the system under study.

Figure 2 shows a typical representation in electrochemical studies, the Nyquist diagram, and the corresponding equivalent circuit used to fit it. The latter is better known with the name of Randles equivalent circuit. The Randles equivalent circuit provided a surprisingly effective simulation of the impedance characteristics of a fast charge transfer reaction at a planar electrode and has been used extensively since its introduction nearly six decades ago [28].

The impedance spectrum profile has a semicircle beginning in the point corresponding to R_1 value (a) and ending in the point (b) corresponding to the sum $R_1 + R_2$ (see Figure 2). The value of capacitance of the capacitor C can be obtained by the maximum value of imaginary impedance in the spectrum. Most of impedance spectra corresponding to electrochemical systems can be fitted to this type of diagram: the parameter R_1 represents the resistance of the solution, R_2 corresponds in most cases to the resistance (R_{ct}) to the charge transfer between the solution and the electrode surface and C is the capacitance of the double layer (due to the interface between the electrode and the electrolytic solution).

The contribution to impedimetric spectrum at low frequencies is represented by the Warburg impedance. This is related to the mass transfer between the solution and the electrode surface and can be modelled as a frequency dependent reactance with equal real and imaginary components.

$$Z_w = \sigma \cdot (\omega)^{-1/2} \cdot (1 - j) \qquad \textbf{(5)}$$

In the equation ω is the radial frequency, and σ the Warburg coefficient (which is constant for a defined system). Although this expression can be used to estimate effective diffusion coefficients of reacting substances, this use is more frequent for fundamental electrochemical studies than for electroanalysis. On a Nyquist plot the Warburg impedance appears as a diagonal line with a slope of 45°.

Another common situation is the non-ideal behaviour of most capacitors in electrochemical systems under study results in impedimetric spectra where the semicircles of Nyquist diagrams present a depressed and not completely symmetric shape. To better fit the experimental data to theoretical curves, the use of a Constant Phase Element (CPE) instead of a capacitor is required [23, 29]. The

impedance of a CPE is given by:

$$Z_{CPE} = (j \cdot \omega)^{-\alpha} / C \quad (6)$$

Where ω is the radial frequency, C the capacitance, and α an empirical coefficient, which is 1 for an ideal capacitor.

For a constant phase element the exponent $\alpha < 1$, since $\alpha = 1$ corresponds to the ideal capacitor. Generally the double layer between the solution and the electrode surface in an electrochemical cell is better fitted by a CPE than a capacitor.

In most cases, due to the complexity of electrochemical system under study, impedimetric spectra and the corresponding equivalent circuits are more complex than the one represented in Figure 2.

An alternative to the complex-plane diagram is the so-called 'Bode diagram', in which log $|Z|$ or the phase angle ϕ are plotted versus log ω. The type of diagram for data representation can be chosen according to different experiments and the need of specific parameter visualization.

Nowadays, EIS has become a mandatory characterization technique to fully understand any electrochemical process at the electrode-electrolyte interface [30]. Although somehow equivalent to a full series of experiments employing the cyclic voltammetry technique at different speeds to scan the potential, the clarity in which EIS yields results in the form of an equivalent circuit and its involved parameters makes it a very attractive technique to describe any electrochemical process.

As mentioned above, impedance spectroscopy is a versatile technique, widely used in different fields' studies, such as corrosion [31, 32] semi-conducting electrodes [33, 34], coatings [35, 36], batteries and fuel cells [37-39] electrochemical kinetics and mechanism [40, 41], biomedical and biological systems [23, 42, 43], electronic and ionic conducting polymers [44, 45], energy [46] or solid-state systems [47].

Due to its ability of directly probing the interfacial properties of a modified electrode, the technique is rapidly developing as a tool for studying biorecognition events at the electrode surface [23, 48-50]. In particular, EIS is becoming an attractive electrochemical tool for numerous applications either in immuno- [51-53] or in genosensing field [16, 54] especially in the last decade.

2. Application of EIS in genosensing

2.1 General overview

The major driving force for studying impedimetric genosensors is their ability to perform label-free

192 detections. Most biosensors require a label attached to the target molecule for the detection, e.g. a
193 redox enzyme or a fluorescence tag. In the case of impedimetric technique, changes in the electrical
194 properties of the surface (e.g. capacitance, resistance) can result solely from the presence of the
195 target molecule. Thus, no label is required for impedance sensing. However, since labelling can
196 increase selectivity (e.g. using sandwich approach with a second probe) and enhance sensitivity (e.g.
197 using a label the can significantly amplify the impedimetric response), some impedance
198 genosensors in the literature use labels with the aim of improving the limit of detection thus
199 avoiding the pre-amplification of the DNA content in the sample by the polymerase chain reaction
200 (PCR).
201 Moreover, the possibility of realizing measurements at a certain single frequency can simplify the
202 equipment required for the measurement. In this case, a simple frequency analyzer (or discrete
203 analyzer at a few numbers of fixed frequencies) can be used instead of the more complex
204 impedimetric apparatus.
205 Hence, impedimetric genosensors [55] are attractive tools due to their potential for simple, rapid,
206 label-free and low cost detection of DNA sequences.
207 Many applications have been presented in literature during the recent years, either including
208 non-Faradic measurements resulting in capacitance sensing [56-64], or employing a redox indicator
209 to monitor resistance changes [65-71] occurring at conductive or semi-conductive surfaces.
210 In the first case the parameter of interest in the study is the capacitance of the double layer formed
211 between the solution and the electrode surface. No additional reagent is required for *non-faradic*
212 *impedance spectroscopy*. In fact, after any further bio-modification of the sensor surface, a variation
213 in the capacitance value can be recorded. This is due to the displacement of water and ions from the
214 surface upon biomolecule binding [40].
215 In the second indirect one, called *faradic impedance spectroscopy*, a redox species, added to the bulk
216 solution, is alternatively oxidized and reduced at the working conductive electrode surface. This
217 process is exploited to observe the variation of charge transfer resistance between the solution and
218 the electrode surface associated to the modification of the latter due to the different steps of the
219 biosensing event. In this case the redox species is considered a marker, not a label, since it will be
220 indirectly related to the sensing event. In the case of genosensors, negatively charged redox species
221 are usually employed. In fact, since nucleic acid/DNA complexes (both single stranded and double
222 stranded DNA) are oligoanionic polymers, their immobilization on surfaces generates a repulsion of
223 the redox marker, thus inhibiting the redox reaction and enhancing the charge transfer resistance
224 value (R_{ct}) [23].
225 In many protocols, in order to enhance the difference in the signal obtained between the probe
226 immobilization and the hybridization with a complementary sequence, a PNA probe is employed
227 instead of DNA [72, 73]. PNA is an artificially synthesized polymer in which the backbone is
228 composed of repeating N-(2-aminoethyl)-glycine units linked by peptide bonds, instead of
229 deoxyribose sugar backbone present in DNA. As PNA is uncharged due to the lack of phosphate

backbone, the R_{ct} variation during the whole biosensing process will be mainly attributable to the hybridization step.

Both *faradic* and *non-faradic impedance spectroscopy* are widely used to different aims, such as:

a) The investigation and characterization of the single layer formed after probe immobilization.
b) The detection of hybridization with a complementary target.
c) The determination of single-nucleotide polymorphism.

Many examples of these different kinds of study are reported in literature.

2.2 Investigation and characterization of the single layer formation after DNA probe immobilization

The first step involved when preparing a genosensor is to immobilize the DNA probe, complementary to the DNA sequence being sought (also known as the DNA target). Strašák et al. [60, 74] exploited the variation of double layer capacitance to monitor the adsorption of both single and double stranded DNA on a hanging mercury drop electrode. Lillis et al. [74] performed single frequency non-faradic impedimetric measurements to compare two different protocols for oligonucleotide probe immobilization, i.e. direct and spacer-mediated attachment of amino modified probe molecules to amino-functionalised surfaces. Lust et al. [75] performed studies of capacitance combined with impedance and chronocoulometry analysis for quantitative characterization of nucleotides adsorption at the bismuth single crystal plane. Brett et al. [76] followed the capacitance changes presented by a glassy carbon electrode covered by a thick film of double stranded DNA, in order to characterize the preparation and conditioning of such sensor surface. Keighley et al. [77] studied the charge screening effect of immobilized DNA probe onto a gold electrode surface by monitoring the charge transfer resistance value. In this way it was possible to optimize the probe surface density for the biosensing event. Lisdat et al. [78] studied the modification of gold electrodes with DNA by self-assembled thiolated oligonucleotides using impedance spectroscopy in the presence of redox couple.

2.3 Detection of hybridization with a complementary target.

The hybridization of the previously immobilized DNA probe with the complementary fragment present in the interrogated sample is obviously the event responsible for the biosensing. This hybridization, normally made manifest by the use of labelling strategies, is directly monitored in the EIS technique, given it will be altering the electrochemical surface characteristics. Oliveira Brett et al. [60] studied either the electrostatic immobilisation onto a glassy carbon electrode of DNA probe oligonucleotides, or the hybridization with complementary target, by monitoring the

difference in the double layer capacitance before and after the modification of the electrode surface. Berggren et al. [56] performed a preliminary study to prove the feasibility of a direct capacitive DNA biosensor for label-free detection of nucleic acids. Gheorghe and Guiseppi-Elie [63] followed the covalent immobilization of DNA probe and the hybridization with a complementary target in a label-free protocol, measuring the total impedance of the system versus the frequency variation. Peng and Travas-Sejdic [66] employed a probe modified copolymer electrode for the detection of DNA hybridization, monitoring the charge transfer resistance variation due to the redox couple ferro/ferricianyde. In this way they were able to distinguish among complementary and non-complementary sequences. Estrela et al. [59] performed capacitance measurements on a metal–insulator–semiconductor (MIS) capacitor for label-free detection of DNA hybridization. In fact, upon hybridization of DNA on the gold gate of a MIS capacitor, the capacitance versus voltage characteristics show a significant shift. Kafka and Lisdat [79] described a label-free detection system for DNA strands based on gold electrodes and impedance measurements. The electrode was impedimetrically characterised in the presence of the redox system ferro/ferricyanide before and after DNA hybridization. Impedance analysis showed that the charge transfer resistance was increasing after DNA duplex formation, whereas the capacitive properties remained rather unaltered. Piro and Gabrielli [80] employed electrochemical impedance spectroscopy for both the characterization of a new bifunctional electroactive polymer, used as a platform for probe immobilization, and the detection of DNA hybridization. Gooding et al. [81] presented a label free electrochemical method of detecting DNA hybridization, based on the change in flexibility between a single strand of DNA and a duplex, causing an ion-gating effect where hybridization opens up the electrode to access of ions. In this way the electron transfer resistance due to the redox marker decreases after the hybridization occurs. Bonanni and del Valle [82] exploited the changes in charge transfer resistance for the detection of hybridization using an avidin-modified graphite epoxy composite as sensing platform. The same authors [83] used impedance spectroscopy together with artificial neural networks to perform a multigenic detection employing a single biosensor with two immobilized DNA probes.

A known drawback of impedimetric biosensors is the potential interaction of other substances on the electrode surface, e.g, non-specific adsorption;, given the high sensitivity of EIS, non-specific adsorption will become manifest in the acquired signal and cause an interference. The alternatives available are to perform full-coverage of electrodes, in a way that no other substances may be adsorbed [84], or to coat the electrode voids with substances that may prevent adsorption of other molecules, per example with polyethylene glycol (PEG) [85, 86]; in both cases, still the biomolecule exchange may be possible, thus reverting the purpose.

Another important issue when dealing with impedimetric biosensors is the representation and comparison of obtained results. In fact, due to the very high sensitivity of the technique, it should take into account that different measurements are generally performed with different electrode units or with the same unit after renewal of the sensing surface. For those reasons results are very

often expressed as the signal variation of the parameter of interest (i.e. charge transfer resistance or capacitance) relative to the value given by the bare electrode. Bonanni and del Valle [70] represented results as the relative R_{ct} variation between the values obtained in the different experiments, i.e. DNA adsorption and hybridization, and R_{ct} value due to the bare electrode. This relative variation is represented as a ratio of delta increments, as sketched on eq. (7).

$$\Delta_{ratio} = \frac{\Delta_s}{\Delta_p} \qquad (7)$$

being $\Delta_s = R_{ct(sample)} - R_{ct(blank)}$ and $\Delta_p = R_{ct(probe)} - R_{ct(blank)}$. This elaboration was required for the comparison of data coming either from different electrode units or for the same unit after surface polishing procedure. Briefly, when hybridization occurred Δ_s/Δ_p value should be > 1 for the hybridization experiments and close to 1 for negative controls with non-complementary targets (that means $\Delta_s = \Delta_p$, i.e. no variation of R_{ct} value because no hybridization occurred).

Peng et al. [87] represent the signal as the normalised sensor response $\Delta R_{ct}/\Delta R_{ct}^0$, where ΔR_{ct}^0 is the change in the charge-transfer resistance of the sensor hybridised with complementary oligonucleotide, whilst ΔR_{ct} is the signal change due to negative controls. In this case $\Delta R_{ct}/\Delta R_{ct}^0$ should approximate 1 in the presence of a complementary target and should be < 1 in the presence of nucleotide polymorphisms or non complementary sequences.

Finally, Kafka et al. [79] represented the impedimetric signal as the ratio of the charge transfer resistance, $R_{ct,h}/R_{ct,d}$, between hybridised (h) and denaturated (d) sensor surfaces after hybridisation with complementary and non-complementary DNA target, which again shows the importance of this normalization.

2.4 Detection of nucleotide polymorphisms

When checking the literature linked to DNA biosensing, many of the developed applications are related to the detection of little variations in specific genes of individuals, per example the change or the deletion of a nucleotide base. This little change in DNA sequence is called a Single Nucleotide Polymorphism, and is of great diagnostic interest. The assay of SNPs is of high significance in the diagnostic of genetic diseases, the respose of organisms to pathogens or drugs, or the establishment of identity of individuals or family relatives.

Bardea and Willner [88] detected the mutant characteristics to the Tay-Sachs genetic disorder comparing the charge transfer resistance values after any further electrode surface modification, in the presence of a redox couple. The hybridization with the complementary mutant was confirmed by performing an amplification step using a biotinylated oligonucleotide. Ito et al. [68] studied single-nucleotide polymorphisms detecting a single-base mismatch at the distal end of target

oligonucleotide. After hybridization with complementary or mismatched DNA, electrochemical impedance spectra were recorded using a redox marker. Hybridization with the complementary DNA reduced the charge-transfer resistance, whereas single-base mismatches at the distal end of the duplex largely increased it. Akagi et al. [89] employed a ligation-based impedimetric DNA sensor for single-nucleotide polymorphism associated with a metabolic syndrome. The use of a specific DNA ligase that bind selectively only to perfectly matched DNA allows the detection of the mismatch. Bonanni et al. [64] employed a gold interdigitated electrode for the detection of the single base mutation in oligonucleotide sequences correlated to BRCA1 (breast cancer) gene.

2.5 Signal amplification

As already mentioned above, despite the rapidity, lower costs and simplicity of label-free protocols, there are situations where maximum sensititivity is of upper importance, for example to reach the lowest detection limits. In this context, the use of labelled oligonucleotides is increasing during the recent years, due to the possibility to improve the genosensor impedimetric response.

Ma and Madou [90] developed an enzymatic amplification scheme employing a biotinylated oligonucleotide to be bound to a streptavidin modified enzyme, in order to increase the sensitivity of the DNA sensor. In this approach, after hybridization, the enzymatic precipitation of an insoluble compound on the sensing interface causes a significant impedance change. In a similar protocol, Patolsky and Willner [91] exploited the biocatalyzed precipitation of an insoluble product on the transducer, to provide a mean to confirm and amplify the detection of a single-base mutation. The sensitivity of the method enabled the quantitative analysis of the mutant of Tay–Sachs genetic disorder without the need of PCR amplification. The same authors [92] employed tagged, negatively charged, liposomes to amplify DNA sensing performance for hybridization and base mismatches detection. Kotler et al. [93] performed an ultrasensitive detection of viral DNA without needing the PCR amplification process prior to the analysis. The method for the analysis of the target viral DNA involved the surface replication and concomitant labelling of the analyzed DNA. Bonanni et al. [94] improved the sensitivity obtained for the detection of SNP correlated to kidney disease by performing the detection in presence of Ca^{2+}. In fact, the specific binding of the metal ions in the presence of A-C nucleotide mismatch induced a further impedance change, thus improving the discrimination between the mutated and healthy gene, as the signal amplification was achieved only for the former.

3. Nanomaterials used in impedimetric genosensing

In the past 10 years, the use of nanoscale materials for electrochemical biosensing has seen

explosive growth. A wide variety of nanoscale materials of different sizes, shapes and compositions are now available [95]. The huge interest in nanomaterials is driven by their many desirable properties. In particular, the ability to tailor the size and structure and hence the properties of nanomaterials offers excellent prospects for designing novel sensing systems [96-98] and enhancing the performance of bioanalytical assays [99-101].

The unique and attractive properties of nanostructured materials present new opportunities for the design of highly sophisticated electroanalytical DNA biosensing devices. Due to their high surface area, nontoxicity, biocompatibility and charge-sensitive conductance they act as effective transducers in nanoscale biosensing and bioelectronic devices. This is especially true when the sensed molecules are on the same order of dimension of the nanocomponents used, as this is the case with DNA. These nanostructured materials based electrochemical DNA devices may present a number of key features, including high sensitivity, exquisite selectivity, fast response time and rapid recovery (reversibility), and potential for integration of addressable arrays on a massive scale, which sets them apart from other sensors technologies available today. The sensitivity of the sensor depends on the dimensions and morphological shape of the nanomaterials involved. Therefore, some morphological (nanotube, nanowires, nanofibers, nanorods) based biosensing transducers could function as effective mediators and facilitate the electron transfer between the active site of probe DNA and surface of the electrodes.

The use of nanomaterials in impedimetric genosensing involves two different aspects. Some works focus on the study and construction of new sensing platforms based on nanoscale materials with the aim of improving the impedimetric response [102-107] (i.e. enhancing the sensitivity of the technique or improving the reproducibility of results). Others are based on the use of DNA oligonucleotides labelled with different types of nanoparticles in order to achieve a significant signal amplification [108, 109]. In fact, the different sterical hindrance and/or electrostatic repulsion generated by presence of nanoparticles onto the electrode surface can strongly influence the impedimetric response [71].

3.1 Nanomaterials used as sensing platform

3.1.1 Carbon based platform: carbon nanotubes and nanostructured diamond

Carbon nanotubes are one of the most commonly used building blocks of nanotechnology [110, 111]. Thanks to their extraordinary properties, like tensile strength, thermal and electrical conductivity or anisotropic behaviour, they are attracting much interest among all applied sciences and technologies. Analytical chemistry is one of the fields taking benefit of several advantages that CNTs bring for applications like chromatography, sensors and biosensors, nanoprobes, etc.

Xu et al. [112, 113] incorporated multi-walled carbon nanotubes (MWCNTs) into composite electrodes used for impedance detection of DNA hybridization with a redox marker. In these studies, MWCNTs were co-polymerized with polypyrrole atop a glassy carbon electrode and then ssDNA was covalently immobilized. The complementary oligonucleotide was detected by the accompanying change in R_{ct}, both with [112] and without 113] subsequent metallization. In the former case an R_{ct} reduction was observed whilst in the latter the value of R_{ct} increased as hybridization occurred. In both cases CNTs were incorporated within the sensing interface due to their high conductivity and their effect of increasing the active surface area. Jiang et al. [114] used a polylysine/single-walled carbon nanotubes modified electrode for the impedimetric detection of transgenic plants gene fragment. The obtained platform presented an enhanced conductivity, with an estimated detection limit around 0.1 pM. Bonanni and del Valle [86] employed screen-printed electrodes modified with carboxyl functionalised multi-walled carbon nanotubes as platforms for impedimetric genosensing of oligonucleotide sequences specific for transgenic insect resistant Bt maize. Amino-modified DNA probe was covalently immobilized by EDC-NHS chemistry. The same authors [115] used the same platform for the very sensitive detection of H1N1 influenza A gene correlated sequence (LOD in the pM range). A similar platform, consisting on carboxylic acid functionalized single walled carbon nanotubes modified graphite sensors was employed by Caliskan and Erdem [116] for electrochemical monitoring of direct DNA hybridization related to specific sequence of Hepatitis B virus. The electrochemical signal resulted enhanced in the presence of carbon nanotubes compared to bare graphite. Voltammetry and impedance spectroscopy studies were performed and compared.

A novel bio-sensing platform was introduced by Nebel et al. [117] by combining a geometrically controlled DNA bonding using vertically aligned diamond nano-wires and the superior electrochemical sensing properties of diamond as transducer material (see Figure 3). Ultra-hard vertically aligned diamond nano-wires were electrochemically modified to bond phenyl linker-molecules to their tips which provide mesospacing for DNA molecules on the transducer. Electro- and bio-chemical sensor properties were investigated using cyclic and differential pulse voltammetry as well as impedance spectroscopy with $Fe(CN)_6^{3-/4-}$ as redox markers, which reveal sensitivities of 2 pM on 3 mm^2 sensor areas and superior DNA bonding stability over 30 hybridization/denaturation cycles.

Vermeeren et al. [118] performed impedance spectroscopy on DNA-functionalized nanocrystalline diamond (NCD) layers during hybridization and denaturation. In both reactions, a difference in behavior was observed for 1-mismatch target DNA and complementary target DNA in real-time, employing a label free format together with a reusable platform.

3.1.2 Nanostructured silicon

Silicon is the ubiquitous material possibiliting computers, cell phones and many other everyday electronic appliances. In the recent years, controlled microfabrication and nanoengineering procedures have been used to give specific shapes and finishings to silicon, looking for specific uses, many of them related to pharmaceutical or biological applications.

Ma et al. [90] fabricated a Nano-SiO_2/p-aminothiophenol (PATP) film for genosensing. EIS was applied to label-free detection of the target DNA according to the increase of the electron transfer resistance (R_{et}) of the electrode surface after the hybridization of the probe DNA with the target DNA. This electrochemical genosensor showed its own performance of simplicity, good stability, fine selectivity and high sensitivity, and was successfully applied to the detection of the PAT gene sequences in a dynamic detection range from 1.0×10^{-11} to 1.0×10^{-6} mol/L 20-base sequence of the phosphinothricin-acetyltransferase (PAT) gene, with the detection limit of 1.5×10^{-12} mol/L. Such DNA sensor had also good ability of recognizing single- or double-base mismatched DNA sequence with the complementary DNA sequence.

Kleps et al. [119] fabricated and optimized different porous silicon (PS) based micro- and nanostructures for biosensing. Meso- and macro-PS have been investigated for DNA biomolecule detection by impedance spectroscopy.

Vamvakaki et al. [120] developed a nanoporous silicon platform to be used as a substrate for the entrapment of oligonucleotides and the subsequent development of stable DNA biosensors. The platform was optimized in order to obtain a surface layer with pore diameters which are close to those of the adsorbed DNA helix. Hybridization efficiency was verified by the large and reproducible impedance changes at the interface layer, in a lebel free protocol.

3.1.3 Gold nanoparticles and nanoelectrodes

Gold nanoparticles are expanding many possibilities in labelling and detection in analytical chemistry. Due to the nanoscopic size, gold nanomaterials display novel physical and chemical properties, such as the nanoscale or surface effects. Catalysis is another enhanced feature that can be employed in synthesis or chemically amplified detection. Apart, gold nanoparticles are redox active nanomaterials, that can be electrochemically detected or give way to detection, what makes them interesting elements for developing electrochemical biosensors. Gold nanoparticles may improve the sensing properties of the biomolecules and also may enhance the electron communication rate between redox active species and electrode surfaces. Additionally, nanoparticles have been recently used as labels in electrochemical DNA sensing [121]: this function is covered below in Sec. 3.2.1.

Fu et al. [102] fabricated a sensing platform by self-assembling a bilayer two-dimensional silane and gold nanoparticles on gold substrate. They successively immobilized HS-ssDNA to the gold nanoparticles. The nanoparticles both inside the network and on the surface increased the surface

area of the modified electrode, which increased the DNA anchor. The DNA biosensor obtained an improved sensitivity in the label-free impedimetric detection of DNA hybridization.

Yang et al. [105] deposited a poly-2,6-pyridinedicarboxylic acid film (PDC) on a glassy carbon electrode (GCE). Then gold nanoparticles (NG) were added to the platform to prepare NG/PDC/GCE. After that ssDNA probe was immobilized on the NG/PDC/GCE by the interaction of NG with DNA. The electron transfer resistance (R_{et}) of the electrode surface in $[Fe(CN)_6]^{3-/4-}$ solution increased after the immobilization of the DNA probe on the NG/PDC/GCE. The hybridization of the DNA probe with cDNA made R_{et} increase further. The NG modified on the PDC dramatically enhanced the immobilization amount of the DNA probe and greatly improved the sensitivity of the label free detection of the sequence-specific DNA related to PAT gene in the transgenic plants. A detection limit of 2.4×10^{-11} mol/L could be estimated.

Bonanni et al. [64] employed gold interdigitated nanoelectrodes exploiting single-frequency capacitance change for the detection of the breast cancer related BRCA1 gene mutation. The nanometric dimensions of the device allowed an improved sensitivity when compared with other similar systems, which enabled a direct, unlabelled detection.

3.1.4 Nanostructured polymers

A further procedure that may be used to obtain nanostructured engineered surfaces is through polymerization in presence of specific substances or arrangements in order to define patterns in the resulting surface. Although this variant is specially suited for sample pretreatment or direct analyte detection, it has also been employed to improve performance of biosensors.

Ghanbari et. al. [103] developed a new biosensor employing an electrochemically fabricated polypyrrole nanofiber-modified electrode [122] for the immobilization by physisorption of dsDNA. The new platform presented an increased electroactivity due to the high specific surface area and a low detection limit for the impedimetric analysis in a label-free protocol.

Feng et al. [104] employed a gold nanoparticle/polyaniline nanotube membranes on a glassy carbon electrode for the impedimetric sensing of the immobilization and hybridization of non-labelled DNA, thus obtaining a much wider dynamic detection range and lower detection limit for the DNA analysis.

Zhang et al. [123] combined the strong adsorption ability of Fe_2O_3 microspheres to DNA probes and excellent conductivity of self-doped polyaniline nanofibers on carbon ionic liquid electrode for electrochemical impedance sensing of the immobilization and hybridization of DNA. The DNA hybridization events were monitored with a label-free EIS strategy. Under optimal conditions, the dynamic range of this DNA biosensor for detecting the sequence-specific DNA of the phosphenolpyruvate carboxylase gene from transgenically modified rape was from 1.0×10^{-13} to 1.0×10^{-7} mol/L, and the detection limit was 2.1×10^{-14} mol/L.

Zhou et al. [124] designed a polyaniline nanofibers (PAN(nano))/carbon paste electrode (CPE) via clopping PAN(nano) in the carbon paste. Afetr that, a nanogold (Au-nano) and carbon nanotubes (CNT) composite nanoparticles were bound on the surface of the PAN(nano)/CPE. The electron transfer resistance (R_{et}) of the electrode surface increased after the immobilization of the probe DNA on the Au-nano-CNT/PAN(nano) films and rose further after the hybridization of the probe DNA. The loading of the DNA probe on Au-nano-CNT/PAN(nano) films was greatly enhanced and the sensitivity for the target DNA detection was markedly improved. The study was applied to the detection of PCR amplified sequences of transgenically modified beans in a label free protocol, achieving a limit of detection of 5.6. x 10^{-13} mol/L.

3.1.5 Nanocomposites and nanomembranes

In recent years, inorganic oxide nanoparticles were used to be the immobilizing carriers of ssDNA probe due to unique properties derived from their low dimensions, large surface area and strong adsorption ability [125]. The integration of those materials into nanocomposites or nanomembranes was realized in order to exploit the synergistic effect of this new nano-matrix which could greatly enhance the loading of ssDNA probes and hence markedly improve the sensitivity of target DNA detection.

Liu et al. [126] developed a biosensing platform for DNA immobilization by modifying glassy carbon electrode with nano-MnO_2/chitosan composite film (MnO_2/CHIT/GCE). The immobilization and hybridization events of DNA were characterized by cyclic voltammetry (CV) and electrochemical impedance spectroscopy (EIS), in a label-free detection. The human immunodeficiency virus (HIV) gene fragment was successfully detected by this DNA electrochemical sensor achieving a detection limit of 1.0×10^{-12} mol/L.

Zhang et al. [127] used a nanocomposite membrane, comprising of nanosized shuttle-shaped cerium oxide (CeO_2), single-walled carbon nanotubes (SWNTs) and hydrophobic room temperature ionic liquid (RTIL) 1-butyl-3-methylimidazolium hexafluorophosphate (BMIMPF6), developed on the glassy carbon electrode for electrochemical sensing of the immobilization and hybridization of DNA. The synergistic effect of nano-CeO_2, SWNTs and RTIL could dramatically enhance the sensitivity of DNA hybridization recognition. The electron transfer resistance (R_{et}) of the electrode surface increased after the immobilization of probe ssDNA on the CeO_2–SWNTs–$BMIMPF_6$ membrane and rose further after the hybridization of the probe ssDNA with its complementary sequence. the detection limit was 2.3×10^{-13} mol/L, in a label free protocol.

The same authors [128] prepared gold nanoparticles (nano Au)/titanium dioxide (TiO_2) hollow microsphere membranes on a carbon paste electrode (CPE) for enhancing the sensitivity of DNA hybridization detection (sse Figure 4a). The hybridization events were monitored with EIS using $[Fe(CN)_6]^{3-/4-}$ as redox marker. The sequence-specific DNA of the 35S promoter from cauliflower

mosaic virus (CaMV35S) gene was detected with this DNA electrochemical sensor. The dynamic detection range was from 1.0×10^{-12} to 1.0×10^{-8} mol/L DNA and a detection limit of 2.3×10^{-13} mol/L could be obtained (see Figure 4b).

3.2 Nanomaterials used as labels for signal amplification

3.2.1 Gold nanoparticles

Moreno-Hagelsieb et al. [109] used a gold nanoparticles labelled oligonucleotide as DNA target in order to amplify the capacitance signal between interdigitated aluminium electrodes imprinted over an oxidized silicon wafer. In addition, a silver enhancement treatment was performed offering a further signal amplification strategy. Bonanni and del Valle [71] used streptavidin-coated gold nanoparticles (strept-AuNPs) to amplify the impedimetric signal generated in a biosensor detecting DNA hybridization event. A biotinylated target sequence was employed to this aim. The obtained impedimetric signal resulted 90% amplified in the presence of strept-AuNPs. In a similar scheme, the same authors [129] performed the detection of double-tagged DNA coming from polymerase chain reaction (PCR) amplification of *Salmonella spp* in real samples. The amplification of impedimetric signal was achieved by the conjugation of the duplex with anti-digoxigenin antibody from mouse. This was followed by a secondary labeling with AuNPs-labelled anti-mouse IgG (Figure 5). Alternatively, an amplification scheme using protein G was also proposed. The achieved limit of detection was in the order of fM, when employing AuNPs labeling.

The detection of cystic fibrosis correlated sequence was also performed by Bonanni et al. [130] using MWCNTs platform and strept-AuNPs amplification in a sandwich scheme. In this work authors compared different protocols for the impedimetric detection of DNA hybridization, finally concluding that with a sandwich scheme the LOD could be improved until 100 pM after signal amplification (see Figures 6 and 7).

3.2.2 Quantum dots

Cadmium sulphide (CdS) nanoparticles have been adopted by Travas-Sejdic et al. [108] to amplify the electrochemical signal after the detection of specific oligonucleotide sequences. The sensor was based on electropolymerization of a conducting polymer (polypyrrole) in the presence of the probe oligonucleotide. The resulting sensing platform was then incubated with the complementary target CdS-labelled oligonucleotide solution. A significant improvement in sensor sensitivity was observed

comparing this system with one where the metal nanoparticles were not used.

Kjällman et al. [131] employed CdTe nanoparticle for the modification of a hairpin DNA probe. The stem–loop structured probes and the blocking poly(ethylene glycol) (PEG) molecules were self-assembled on the gold electrode through S–Au bonding, to form a mixed monolayer employed as the sensing platform (see Figure 7). Impedance spectroscopy was used for investigation of the electron transfer processes at a modified gold electrode before and after hybridization with the target DNA. The sensor showed reliable and sensitive detection of 4.7 fM of target and discrimination of non-complementary targets was also achieved.

Xu et al. [132] covalently immobilized DNA probes onto a self-assebled mercaptoacetic acid monolayer modified gold electrode; then, after hybridization with the target ssDNA-CdS nanoconjugate, they observed a remarkably increased R_{ct} value only when complementary DNA sequence was used compared with three-base mismatched or non-completely matched sequences. The results showed that CdS nanoparticle labels on target DNA improved the sensitivity of two orders of magnitude when compared with non-labelled DNA sequences.

3.3 Summary of employed materials and applications

Table 1 show a summery of employed nanomaterials and applications of above mentioned impedimetric genosensors. As we can see, several applications are correlated to the detection of transgenic plants and genetically modified organisms [86, 104, 105, 114, 124]. Other important applications, regarding the medical field, include the identification of certain gene or nucleotide polymorphism correlated to specific disease [64, 109, 115, 117, 126, 130].

4. Future perspectives

Impedimetric genosensors is nowadays an active research area, where many formats and designs are proposed in order to achieve better biosensing features. Further research should be mainly focused on the improvement of their reproducibility and stability. Moreover, scientists still should increase efforts to optimize the proposed electrode assemblies for use in real samples, overcoming all problems associated with the complexity of matrices in various natural or commercial samples. Fulfilment of these analytical parameters will accelerate their passage to routine use, and may even enable the construction of analytical devices based on this philosophy.

Electrochemical impedance sensors are particularly promising for portable, on-site applications, in combination with simplified discrete-frequency instruments. In addition, impedance technique is fully compatible with multiplexed detections in electrically addressable DNA chips, which is one of

the clear demands in genosensing for the next years. However, a future application in these fields, together with the commercialization of a useful device will depend on improvements in several different areas, including minimization of the effects of non-specific adsorption.

All what has been commented in this review is also extensible to specific detection of proteins, in this case taking advantage of the DNA-protein interaction exploited by aptamer sensors [133]. In analogy to the protocols described before, electrochemical impedance spectroscopy can also be employed as detection technique.

5. Conclusions

We have briefly reviewed current improvements described in DNA sensors employing EIS as the detection principle.EIS has been widely used to investigate a variety of electrochemical systems, including fundamental redox studies, corrosion, electrodeposition, batteries and fuel cells. However, only recently impedance methods have been applied in the field of biosensors. Given their ability to monitor R_{ct} and C_d, application should be possible for several different types of sensing schemes, with numerous recognition agents, by direct signal acquisition, or with the use of simple and cheap redox markers. In this sense, impedimetric genosensors can potentially accomplish label-free assays. In general, impedimetric genosensors are extremely simple in operation, and capable of achieving low detection limits even when used without any amplification. If combined with additional signal amplification strategies, their absolute detection limits may be comparable to any other genosensor type. The contribution of nanostructured materials in its development is a timely area of activity, whether they may be used as sensing platform, or, once hybridization has occurred, in additional amplification stages.

Acknowledgements

Financial support for this work has been provided by the Ministry of Science and Technology (MCyT, Madrid, Spain) through projects Consolider-Ingenio CSD2006-00012 and TEC2007-68012-C03-02/MIC, and by the Department of Innovation, Universities and Enterprise (DIUE) from the Generalitat de Catalunya.

References

[1] S. Cosnier, P. Mailley, Analyst 133 (2008) 984-991.
[2] T.G. Drummond, M.G. Hill, J.K. Barton, Nat. Biotechnol. 21 (2003) 1192-1199.
[3] P.G. Righetti, C. Gelfi, Electrophoresis 18 (1997) 1709-1714.
[4] M.I. Pividori, S. Alegret, Anal. Lett. 36 (2003) 1669-1695.
[5] P.A.E. Piunno, U.J. Krull, R.H.E. Hudson, M.J. Damha, H. Cohen, Anal. Chem. 67 (1995) 2635-2643.
[6] C.H. Fan, K.W. Plaxco, A.J. Heeger, P. Natl. Acad. Sci. Usa 100 (2003) 9134-9137.
[7] A. Lermo, S. Campoy, J. Barbe, S. Hernandez, S. Alegret, M. Pividori, Biosens. Bioelectron. 22 (2007) 2010-2017.
[8] M. Díaz-González, A. de la Escosura-Muñiz, M.B. González-García, A. Costa-García, Biosens. Bioelectron. 23 (2008) 1340-1346.
[9] H.A. Ferreira, F.A. Cardoso, R. Ferreira, S. Cardoso, P.P. Freitas, J. Appl. Phys. 99 (2006).
[10] J. Wang, D.K. Xu, A.N. Kawde, R. Polsky, Anal. Chem. 73 (2001) 5576-5581.
[11] J. Wang, G. Liu, R. Polsky, A. Merkoçi, Electrochem. commun. 4 (2002) 722-726.
[12] K.M. Millan, A. Saraullo, S.R. Mikkelsen, Anal. Chem. 66 (1994) 2943-2948.
[13] K. Maruyama, J. Motonaka, Y. Mishima, Y. Matsuzaki, I. Nakabayashi, Y. Nakabayashi, Sens. Actuat. B 76 (2001) 215-219.
[14] F. Yan, A. Erdem, B. Meric, K. Kerman, M. Ozsoz, O.A. Sadik, Electrochem. Commun. 3 (2001) 224-228.
[15] K. Hashimoto, K. Ito, Y. Ishimori, Anal. Chem. 66 (1994) 3830-3833.
[16] F. Lisdat, D. Schafer, Anal. Bioanal. Chem. 391 (2008) 1555-1567.
[17] J. Wang, A.B. Kawde, Analyst 127 (2002) 383-386.
[18] H.H. Thorp, Tren. Biotechnol. 16 (1998) 117-121.
[19] C.K. O'Sullivan, G.G. Guilbault, Biosens. Bioelectron. 14 (1999) 663-670.
[20] M. Lazerges, H. Perrot, N. Zeghib, E. Antoine, C. Compere, Sens. Actuat. B 120 (2006) 329-337.
[21] P. Schuck, Annu. Rev. Bioph. Biom. 26 (1997) 541-566.
[22] J. Homola, S.S. Yee, G. Gauglitz, Sens. Actuat. B 54 (1999) 3-15.
[23] E. Katz, I. Willner, Electroanalysis 15 (2003) 913-947.
[24] H.J. Josephs, "The Heaviside Papers found at Paignton in 1957". Electromagnetic Theory by Oliver Heaviside., New York, Chelsea Publishing Co., 1971.
[25] J.R. Macdonald, Impedance Spectroscopy, New York, Wiley, 1987.
[26] A.J. Bard, L.R. Faulkner, Electrochemical Methods, New York, Wiley, 1980.
[27] M. Sluyters-Rehbach, J.H. Sluyters, Electroanalytical Chemistry, New York, Marcel Dekker, 1970.
[28] J.E.B. Randles, Discuss. Faraday Soc. 1 (1947) 11-19.
[29] H. Cai, Y. Xu, N.N. Zhu, P.G. He, Y.Z. Fang, Analyst 127 (2002) 803-808.
[30] S.M. Park, J.S. Yoo, Anal. Chem. 75 (2003) 455A-461A.
[31] F. Mansfeld, L.T. Han, C.C. Lee, C. Chen, G. Zhang, H. Xiao, Corros. Sci. 39 (1997) 255-279.
[32] N. Srisuwan, N. Ochoa, N. Pebere, B. Tribollet, Corros. Sci. 50 (2008) 1245-1250.
[33] A.A. Sagues, J.T. Wolan, A. De Fex, T.J. Fawcett, Electrochim. Acta 51 (2006) 1656-1663.
[34] E. Sosa, R. Cabrera-Sierra, M.T. Oropeza, F. Hernandez, N. Casillas, R. Tremont, C. Cabrera, I. Gonzalez, Electrochim. Acta 48 (2003) 1665-1674.
[35] B. Tzvetkov, M. Bojinov, A. Girginov, N. Pebere, Electrochim. Acta 52 (2007) 7724-7731.
[36] A. Nogueira, X.R. Novoa, C. Perez, Prog. Org. Coat. 59 (2007) 186-191.
[37] A.K. Manohar, O. Bretschger, K.H. Nealson, F. Mansfeld, Bioelectrochemistry 72 (2008) 149-154.
[38] S.K. Roy, M.E. Orazem, J. Power Sources 184 (2008) 212-219.
[39] N. Wagner, Electrochemical power sources-Fuel cells, New York, Wiley, 2005.
[40] F. Seland, R. Tunold, D.A. Harrington, Electrochim. Acta 51 (2006) 3827-3840.
[41] R.D. Amstrong, M.F. Bell, A.A. Metcalfe, Special Periodical Reports-Electrochemistry 6, 1978, 98-127.
[42] A.B. Kharitonov, L. Alfonta, E. Katz, I. Willner, J. Electroanal. Chem. 487 (2000) 133-141.
[43] J.S. Daniels, N. Pourmand, Electroanalysis 19 (2007) 1239-1257.
[44] C. Gabrielli, J.J. Garcia-Jareno, M. Keddam, H. Perrot, F. Vicente, J. Phys. Chem. B 106 (2002) 3182-3191.
[45] P. Sistat, A. Kozmai, N. Pismenskaya, C. Larchet, G. Pourcelly, V. Nikonenko, Electrochim. Acta 53 (2008) 6380-6390.

[46] M. Thele, J. Schiffer, E. Karden, E. Surewaard, D.U. Sauer, J. Power Sources 168 (2007) 31-39.
[47] D. Vladikova, G. Raikova, Z. Stoynov, H. Takenouti, J. Kilner, S. Skinner, Solid State Ionics 176 (2005) 2005-2009.
[48] C. Berggren, B. Bjarnason, G. Johansson, Electroanalysis 13 (2001) 173-180.
[49] C. Gabrielli, Use and Application of Electrochemical Impedance Techniques, Farnborough, UK, Solartron Analytical, 1990.
[50] D.B. Kell, C L Davey Conductimetric and impedance devices, in Biosensors. A practical approach., Oxford, UK, IRL Press, 1990.
[51] H. Huang, Z. Liu, X. Yang, Anal. Biochem. 356 (2006) 208-214.
[52] I. Willner, B. Willner, Biotechnol. Prog. 15 (1999) 991-1002.
[53] C. Tlili, H. Korri-Youssoufi, L. Ponsonnet, C. Martelet, N.J. Jaffrezic-Renault, Talanta 68 (2005) 131-137.
[54] J.Y. Park, S.M. Park, Sensors 9 (2009) 9513-9532.
[55] A. Guiseppi-Elie, L. Lingerfelt, in, Immobilisation of DNA on Chips I, 2005, pp. 161-186.
[56] C. Berggren, P. Stalhandske, J. Brundell, G. Johansson, Electroanalysis 11 (1999) 156-160.
[57] F. Wei, B. Sun, Y. Guo, X.S. Zhao, Biosens. Bioelectron. 18 (2003) 1157-1163.
[58] L. Moreno-Hagelsieb, B. Foultier, G. Laurent, R. Pampin, J. Remacle, J.P. Raskin, D. Flandre, Biosens. Bioelectron. 22 (2007) 2199-2207.
[59] P. Estrela, P. Migliorato, H. Takiguchi, H. Fukushima, S. Nebashi, Biosens. Bioelectron. 20 (2005) 1580-1586.
[60] A.M. Oliveira Brett, A.M. Chiorcea Paquim, V. Diculescu, T.S. Oretskaya, Bioelectrochemistry 67 (2005) 181-190.
[61] H. Berney, J. West, E. Haefele, J. Alderman, W. Lane, J.K. Collins, Sens. Actuat. B 68 (2000) 100-108.
[62] L. Strasák, J. Dvorák, S. Hason, V. Vetterl, Bioelectrochemistry 56 (2002) 37-41.
[63] M. Gheorghe, A. Guiseppi-Elie, Biosens. Bioelectron. 19 (2003) 95-102.
[64] A. Bonanni, I. Fernández-Cuesta, X. Borrisé, F. Pérez-Murano, S. Alegret, M.d. Valle, Microchim. Acta.
[65] G. Farace, G. Lillie, T. Hianik, P. Payne, P. Vadgama, Bioelectrochemistry 55 (2002) 1-3.
[66] H. Peng, C. Soeller, N. Vigar, P.A. Kilmartin, M.B. Cannell, G.A. Bowmaker, R.P. Cooney, J. Travas-Sejdic, Biosens. Bioelectron. 20 (2005) 1821-1828.
[67] Z.-l. Zhi, V. Drazan, O.S. Wolfbeis, V.M. Mirsky, Bioelectrochemistry 68 (2006) 1-6.
[68] T. Ito, K. Hosokawa, M. Maeda, Biosens. Bioelectron. 22 (2007) 1816-1819.
[69] V. Dharuman, T. Grunwald, E. Nebling, J. Albers, L. Blohm, R. Hintsche, Biosens. Bioelectron. 21 (2005) 645-654.
[70] A. Bonanni, M.J. Esplandiu, M.I. Pividori, S. Alegret, M. del Valle, Anal. Bioanal. Chem. 385 (2006) 1195-1201.
[71] A. Bonanni, M.J. Esplandiu, M. del Valle, Electrochim. Acta 53 (2008) 4022-4029.
[72] T.H. Degefa, J. Kwak, J. Electroanal. Chem. 612 (2008) 37-41.
[73] J.Y. Liu, S.J. Tian, P.E. Nielsen, W. Knoll, Chem. Commun. (2005) 2969-2971.
[74] B. Lillis, M. Manning, E. Hurley, H. Berney, R. Duane, A. Mathewson, M.M. Sheehan, Biosens. Bioelectron. 22 (2007) 1289-1295.
[75] E. Lust, A. Janes, K. Lust, J. Electroanal. Chem. 449 (1998) 153-163.
[76] C.M.A. Brett, A.M. Oliveira Brett, S.H.P. Serrano, Electrochim. Acta 44 (1999) 4233-4239.
[77] S.D. Keighley, P. Li, P. Estrela, P. Migliorato, Biosens. Bioelectron. 23 (2008) 1291-1297.
[78] F. Lisdat, B. Ge, B. Krause, A. Ehrlich, H. Bienert, F.W. Scheller, Electroanalysis 13 (2001) 1225-1230.
[79] J. Kafka, O. Pänke, B. Abendroth, F. Lisdat, Electrochim. Acta 53 (2008) 7467-7474.
[80] B. Piro, J. Haccoun, M.C. Pham, L.D. Tran, A.Rubin, H. Perrot, C. Gabrielli, J. Electroanal. Chem. 577 (2005) 155-165.
[81] J.J. Gooding, A. Chou, F.J. Mearns, E. Wong, K.L. Jericho, Chem. Commun. (2003) 1938-1939.
[82] A. Bonanni, M.I. Pividori, M. del Valle, Anal. Bioanal. Chem. 389 (2007) 851-861.
[83] A. Bonanni, D. Calvo, M. del Valle, Electroanalysis 20 (2008) 941-948.
[84] A. Erdem, M.I. Pividori, M. del Valle, S. Alegret, J. Electroanal. Chem. 567 (2004) 29-37.
[85] J. Lahiri, L. Isaacs, J. Tien, G.M. Whitesides, Anal. Chem. 71 (1999) 777-790.
[86] A. Bonanni, M.J. Esplandiu, M. del Valle, Biosens. Bioelectron. 24 (2009) 2885-2891.
[87] H. Peng, C. Soeller, N.A. Vigar, V. Caprio, J. Travas-Sejdic, Biosens. Bioelectron. 22 (2007) 1868-1873.
[88] A. Bardea, F. Patolsky, A. Dagan, I. Willner, Chem. Commun. (1999) 21-22.

[89] Y. Akagi, M. Makimura, Y. Yokoyama, M. Fukazawa, S. Fujiki, M. Kadosaki, K. Tanino, Electrochim. Acta 51 (2006) 6367-6372.
[90] K.-S. Ma, H. Zhou, J. Zoval, M. Madou, Sens. Actuat. B 114 (2006) 58-64.
[91] F. Patolsky, A. Lichtenstein, I. Willner, Nat. Biotechnol. 19 (2001) 253-257.
[92] F. Patolsky, A. Lichtenstein, I. Willner, J. Am. Chem. Soc. 123 (2001) 5194-5205.
[93] F. Patolsky, A. Lichtenstein, M. Kotler, I. Willner, Angew. Chem. Int. Edit. 40 (2001) 2261-2265.
[94] A. Bonanni, M. Pumera, Y. Miyahara, Anal. Chem. 82 3772-3779.
[95] C.P. Poole, F.J. Owens, Introduction to Nanotechnology, New York, Wiley, 2003.
[96] J. Wang, Analyst 130 (2005) 421-426.
[97] J. Wang, Electroanalysis 17 (2005) 7-14.
[98] A. Merkoçi, M. Pumera, X. Llopis, B. Pérez, M. del Valle, S. Alegret, Trends Analyt. Chem. 24 (2005) 826-838.
[99] E. Katz, I. Willner, J. Wang, Electroanalysis 16 (2004) 19-44.
[100] X.L. Luo, A. Morrin, A.J. Killard, M.R. Smyth, Electroanalysis 18 (2006) 319-326.
[101] I. Suni, Trends Analyt. Chem. 27 (2008) 604-611.
[102] Y.Z. Fu, R. Yuan, L. Xu, Y.Q. Chai, X. Zhong, D.P. Tang, Biochem. Eng. J. 23 (2005) 37-44.
[103] K. Ghanbari, S.Z. Bathaie, M.F. Mousavi, Biosens. Bioelectron. 23 (2008) 1825-1831.
[104] Y. Feng, T. Yang, W. Zhang, C. Jiang, K. Jiao, Anal. Chim. Acta 616 (2008) 144-151.
[105] J. Yang, T. Yang, Y. Feng, K. Jiao, Anal. Biochem. 365 (2007) 24-30.
[106] X. Lin, G. Kang, L. Lu, Bioelectrochemistry 70 (2007) 235-244.
[107] M. Guo, J. Chen, D. Liu, L. Nie, S. Yao, Bioelectrochemistry 62 (2004) 29-35.
[108] H. Peng, C. Soeller, M.B. Cannell, G.A. Bowmaker, R.P. Cooney, J. Travas-Sejdic, Biosens. Bioelectron. 21 (2006) 1727-1736.
[109] L. Moreno-Hagelsieb, P.E. Lobert, R. Pampin, D. Bourgeois, J. Remacle, D. Flandre, Sens. Actuat. B 98 (2004) 269-274.
[110] L. Agui, P. Yanez-Sedeno, J.M. Pingarron, Anal. Chim. Acta 622 (2008) 11-47.
[111] A. Merkoci, Microchim. Acta 152 (2006) 157-174.
[112] Y. Xu, Y. Jiang, H. Cai, P.G. He, Y.Z. Fang, Anal. Chim. Acta 516 (2004) 19-27.
[113] Y. Xu, X.Y. Ye, L. Yang, P.A. He, Y.Z. Fang, Electroanalysis 18 (2006) 1471-1478.
[114] C. Jiang, T. Yang, K. Jiao, H.W. Gao, Electrochim. Acta 53 (2008) 2917-2924.
[115] A. Bonanni, M.I. Pividori, M.d. Valle, Analyst (2010), DOI:10.1039/C000532K.
[116] A. Caliskan, A. Erdem, H. Karadeniz, Electroanalysis 21 (2009) 2116-2124.
[117] C.E. Nebel, N. Yang, H. Uetsuka, E. Osawa, N. Tokuda, O. Williams, Diam. Relat. Mater. 18 (2009) 910-917.
[118] V. Vermeeren, N. Bijnens, S. Wenmackers, M. Daenen, K. Haenen, O.A. Williams, M. Ameloot, A. Vandeven, P. Wagner, L. Michiels, Langmuir 23 (2007) 13193-13202.
[119] I. Kleps, M. Miu, M. Simion, T. Ignat, A. Bragaru, F. Craciunoiu, M. Danila, J. Biomed. Nanotechnol. 5 (2009) 300-309.
[120] V. Vamvakaki, N.A. Chaniotakis, Electroanalysis 20 (2008) 1845-1850.
[121] S.J. Guo, E.K. Wang, Anal. Chim. Acta 598 (2007) 181-192.
[122] V. Pichon, F. Chapuis-Hugon, Anal. Chim. Acta 622 (2008) 48-61.
[123] W. Zhang, T. Yang, X. Li, D.B. Wang, K. Jiao, Biosens. Bioelectron. 25 (2009) 428-434.
[124] N. Zhou, T. Yang, C. Jiang, M. Du, K. Jiao, Talanta 77 (2009) 1021-1026.
[125] Y.H. Yang, Z.J. Wang, M.H. Yang, J.S. Li, F. Zheng, G.L. Shen, R.Q. Yu, Anal. Chim. Acta 584 (2007) 268-274.
[126] Z.M. Liu, Z.J. Li, G.L. Shen, R.Q. Yu, Anal. Lett. 42 (2009) 3046-3057.
[127] W. Zhang, T. Yang, X.M. Zhuang, Z.Y. Guo, K. Jiao, Biosens. Bioelectron. 24 (2009) 2417-2422.
[128] Y.C. Zhang, T. Yang, N. Zhou, W. Zhang, K. Jiao, Sci. China B 51 (2008) 1066-1073.
[129] A. Bonanni, M.I. Pividori, S. Campoy, J. Barbe, M. del Valle, Analyst 134 (2009) 602-608.
[130] A. Bonanni, M.J. Esplandiu, M.d. Valle, Biosens. Bioelectron. submitted (2010).
[131] T.H.M. Kjallman, H. Peng, C. Soeller, J. Travas-Sejdic, Analyst 135 (2010) 488-494.
[132] Y. Xu, H. Cai, P.G. He, Y.Z. Fang, Electroanalysis 16 (2004) 150-155.
[133] A.E. Radi, J.L.A. Sanchez, E. Baldrich, C.K. O'Sullivan, Anal. Chem. 77 (2005) 6320-6323.

CAPTIONS FOR FIGURES

Figure 1. AC excitation signal applied and sinusoidal current response in the system under study.

Figure 2. Nyquist diagram and the corresponding equivalent Randles circuit.

Figure 3. a) Phenyl linker molecules are preferentially attached to tips of wires due to the electrochemical attachment schema. b) After phenyl-linker molecules bonded to the tips of wires, the hetero-bifunctional cross linker and CK20 cancer marker DNA will bond according to the geometrical properties of wires (with permission from [117]).

Figure 4. A) SEM images of TiO_2 hollow microspheres synthesized at pH 6.0－7.0 at 180°C for 24 h using titanium powder as Ti source. B) Nyquist diagrams at (1) probe ssDNA/nano Au/ TiO_2/CPE and after hybridization reaction with different concentrations of the target DNA: (2) 1.0×10^{-12}, (3) 1.0×10^{-11}, (4) 1.0×10^{-10}, (5) 1.0×10^{-9}, (6) 1.0×10^{-8} mol/L. Supporting electrolyte solution is 2.5 mmol/L $[Fe(CN)6]^{3-/4-}$ (1:1) + 0.1 mol/L KCl (from [128] with kind permission of Springer Science and Business Media).

Figure 5. Schematic representation of experimental protocol. A) Representation of the avidin modified electrode and its surface. B) Immobilization of double labelled IS200 amplicon on the electrode surface trough the formation of biotin-avidin complex. C1) Addition of aM-gold-Ab/anti-DIG complex. C2) Addition of protein G (with permission from [129]).

Figure 6. Schematic of experimental protocol (with permission from [130]).

Figure 7. Histogram representing results obtained for hybridization experiments with: mutant (complementary target); wild: 3-mismatched target; nc: non complementary sequence for negative control. Reported values correspond to DNA target concentration of 3 pmol (in 13 µl solution). $\Delta_{ratio}= \Delta_g/\Delta_p$; $\Delta_s = R_{ct(sample)} - R_{ct(blank)}$; $\Delta_p = R_{ct(probe)} - R_{ct(blank)}$. Error bars correspond to triplicate experiments. Nyquist plots were obtained in 0.1 PBS buffer solution containing 10 mM $K_3[Fe(CN)_6]/K_4[Fe(CN)_6]$ (with permission from [130]).

Figure 8. Schematic illustration of the fabrication of the sensor: (1) immobilization of HPP and PEG molecules to the gold electrode, (2) attachment of CdTe NPs through an amide bond and (3) hybridization with complementary DNA. (with permission of [131]).

Table 1

Table 1. Summary of employed nanomaterials and applications with impedimetric genosensors recorded in the literature.

Working electrode	Nanocomponent used	Application	LOD	Reference
Al/Al_2O_3	AuNPs	Cytochrome P450 2p2 gene	2 pM	[58]
Interdigiteated nanogold	AuNPs	Breast cancer gene (BRCA1)	150 nM	[64]
Graphite-epoxy composite	AuNPs	Arbitrary sequence (not specified)	120 nM	[71]
MWCNTs	AuNPs	Transgenic maize	2 nM	[86]
gold	AuNPs	Arbitrary sequence (not specified)	5 nM	[102]
Glassy carbon	AuNPs/polyaniline nanotubes	PAT gene (transgenic crops)	300 fM	[104]
Glassy carbon	AuNPs	PAT gene	24 pM	[105]
gold	CdS nanoparticles	Arbitrary sequence (not specified)	1 nM	[108]
Al/Al_2O_3	AuNPs	HIV gene	200 pM	[109]
Glassy carbon	MWCNTs	Arbitrary sequence (not specified)	50 pM	[112]
Glassy carbon	MWCNTs	-	5 pM	[113]
Carbon paste	SWCNTs	PAT and NOS genes	300 fM	[114]
MWCNTs	AuNPs	Influena A virus H_1N_1 gene	500 nM	[115]
diamond	Diamond nanowires	cancer marker cytokeratin 20	2 pM	[117]
carbon ionic liquid electrode	polyaniline nanofibers	phosphenolpyruvate carboxylase (PEPCase) gene	20 fM	[123]
Carbon paste	polyaniline nanofibers, AuNPs, CNTs	transgenically modified beans	500 fM	[124]
Glassy carbon	Nano-MnO_2/chitosan	HIV gene	1 pM	[126]
Glassy carbon	CeO_2 nanoparticles, SWCNTs	(PEPCase) gene	200 fM	[127]
Carbon paste	AuNPs/TiO_2	Cauliflower mosaic virus gene	200 fM	[128]
Avidin graphite-epoxy biocomposite	AuNPs	Salmonella spp IS200 fragment	400 fM	[129]
MWCNTs	AuNPs	Cystic fibrosis gene related sequence	100 pM	[130]
gold	CdTe nanoparticles	Arbitrary sequence (not specified)	5 fM	[131]
gold	CdS nanoparticles	-	-	[132]

Figure 1
Click here to download Figure: Fig1.pdf

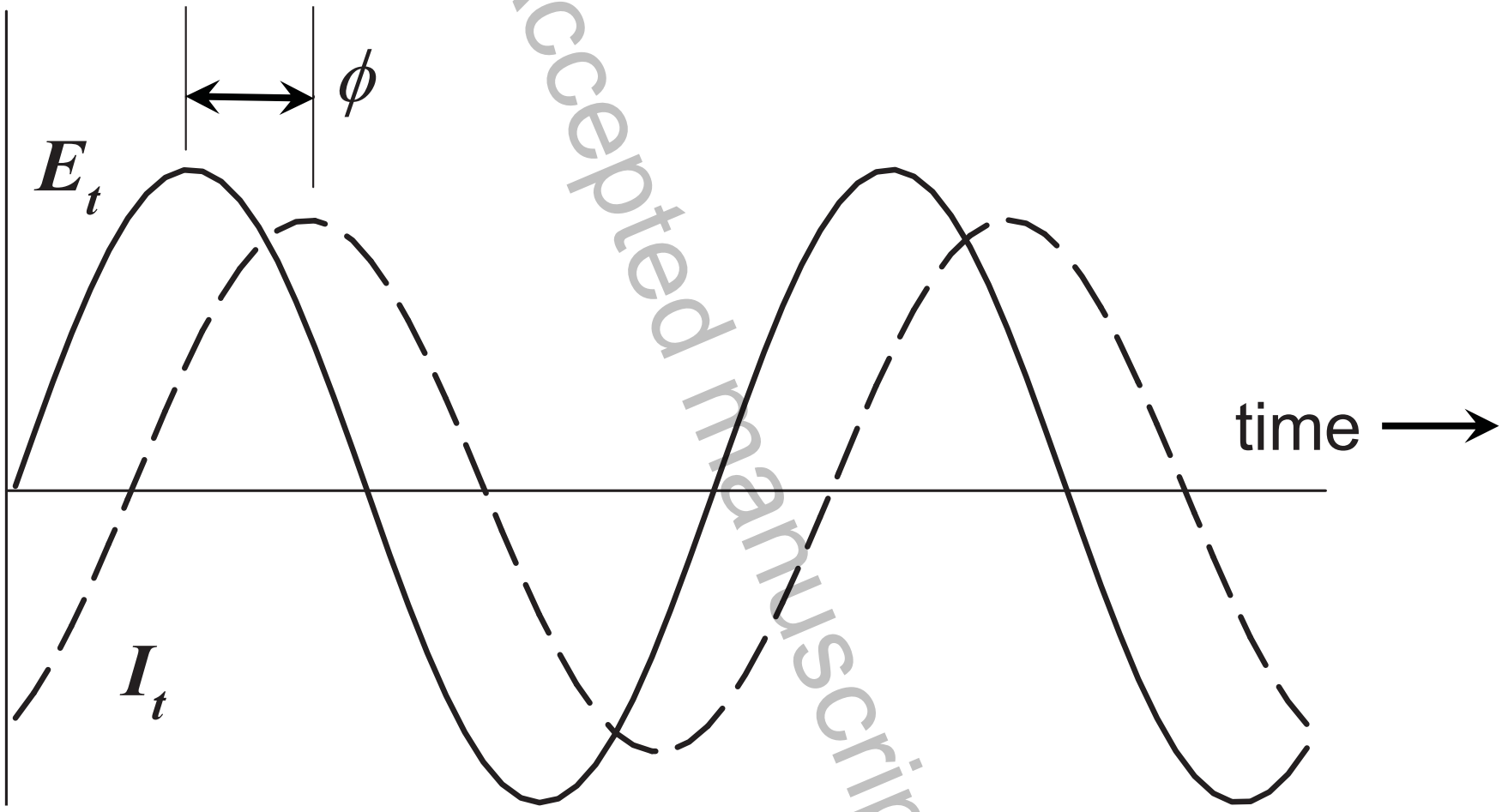

Figure 2
Click here to download Figure: FIG2.pdf

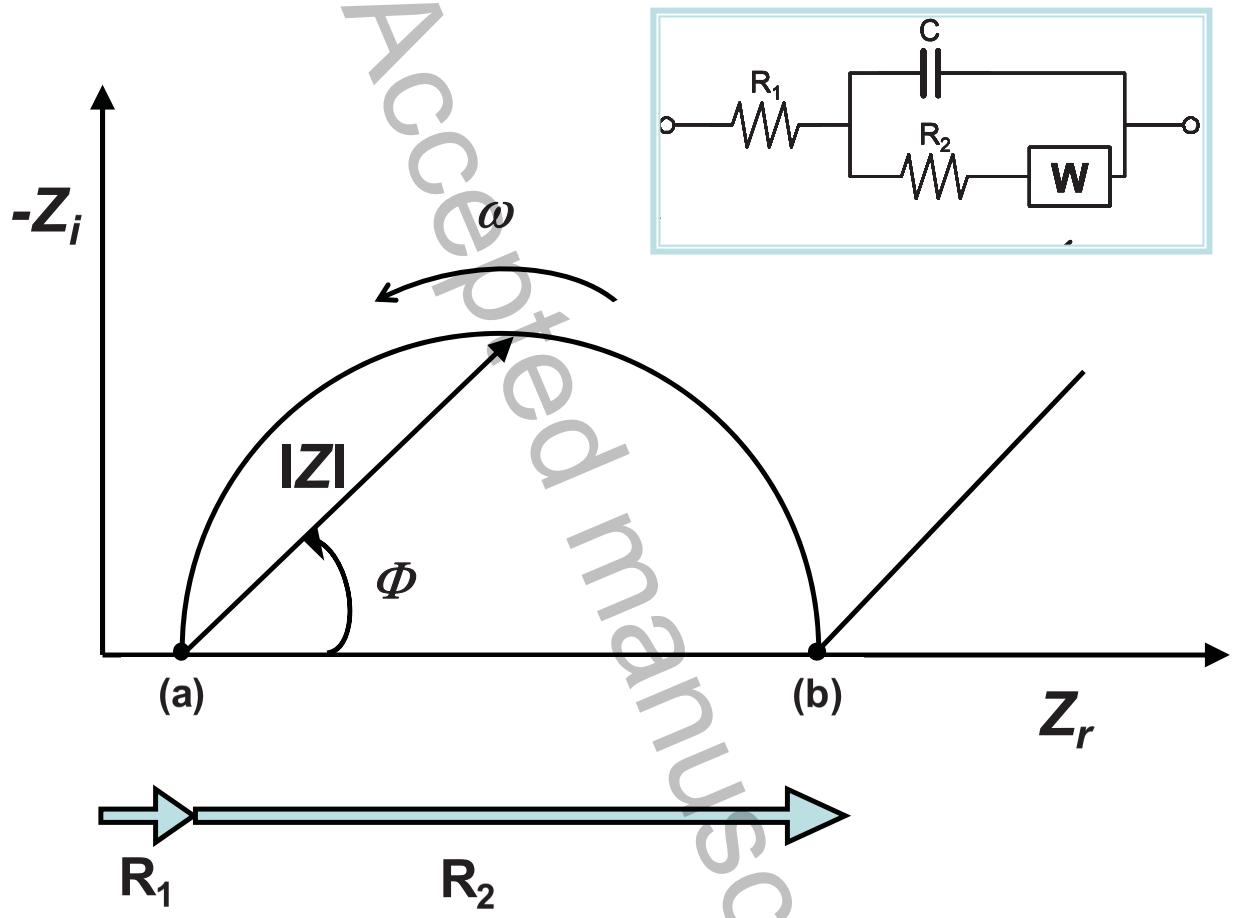

Figure 2

Figure 3

Click here to download Figure: FIG3.pdf

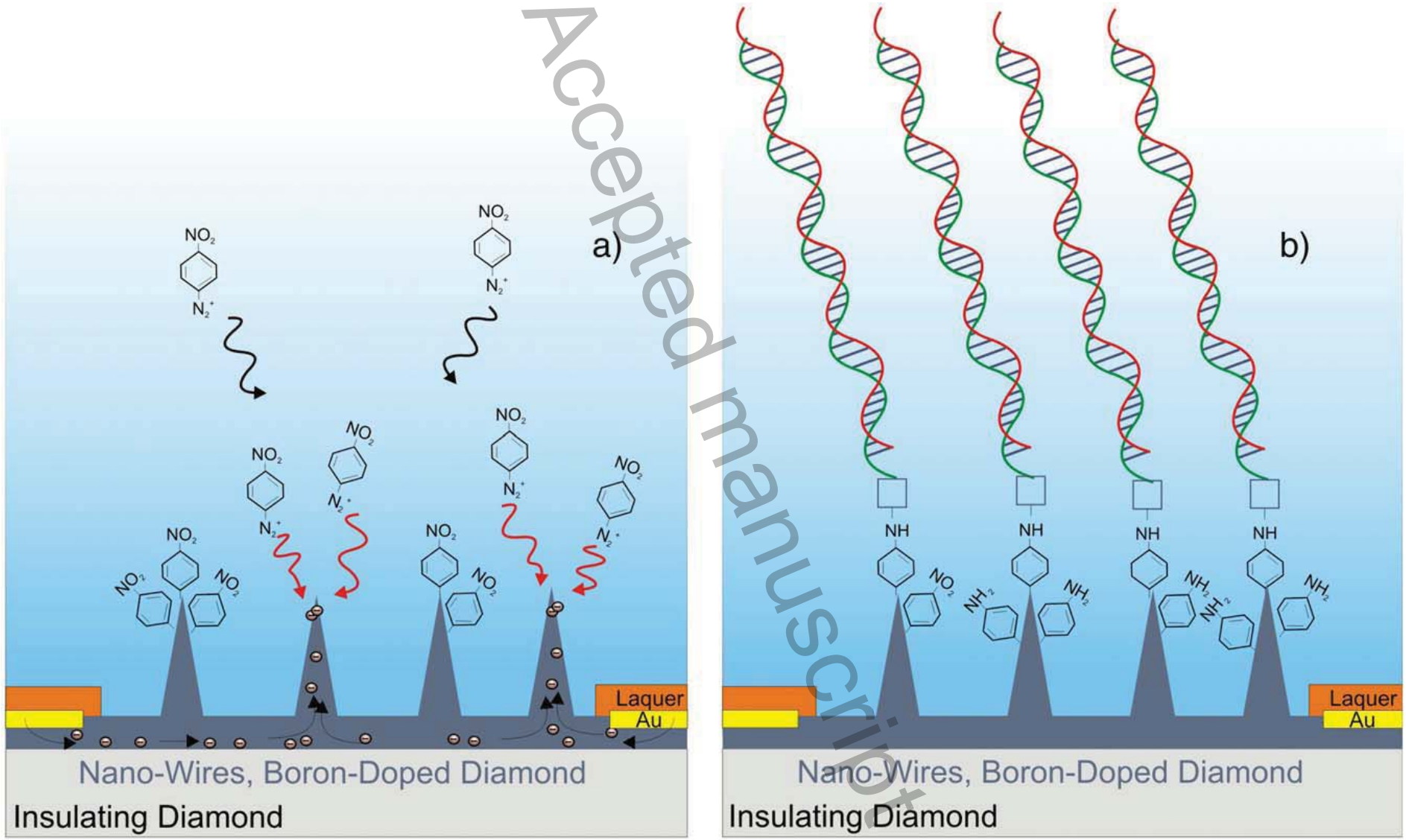

Figure 4
Click here to download Figure: FIG4.pdf

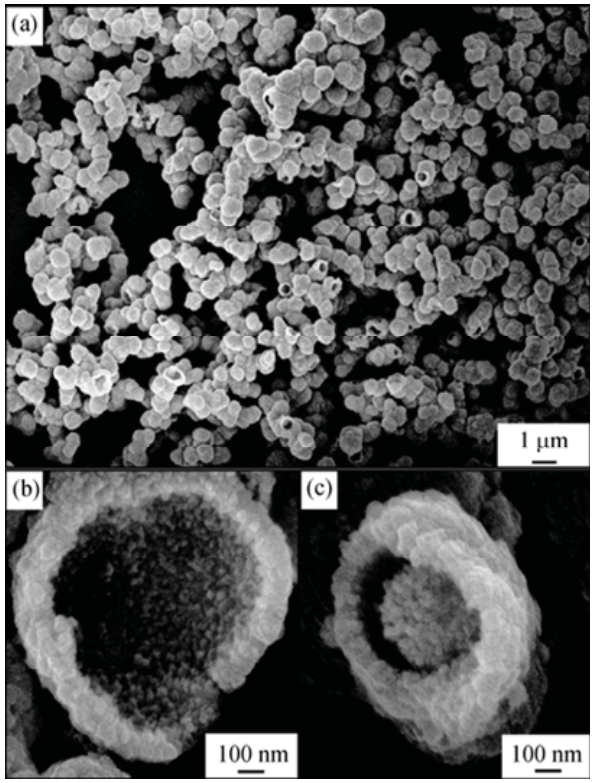

A

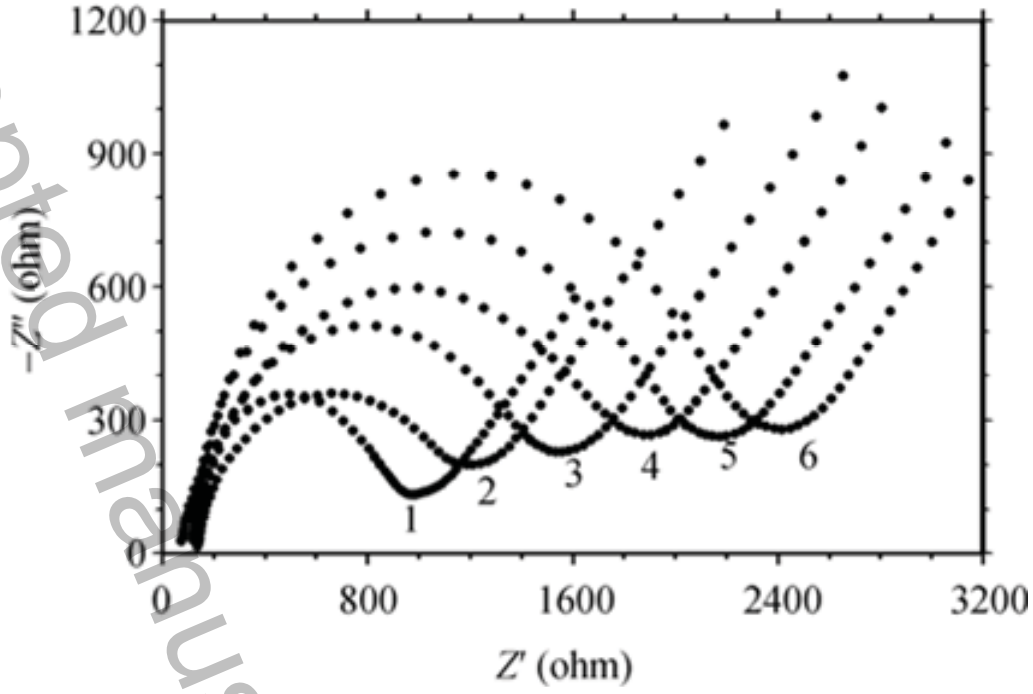

B

Figure 5
Click here to download Figure: FIG5.pdf

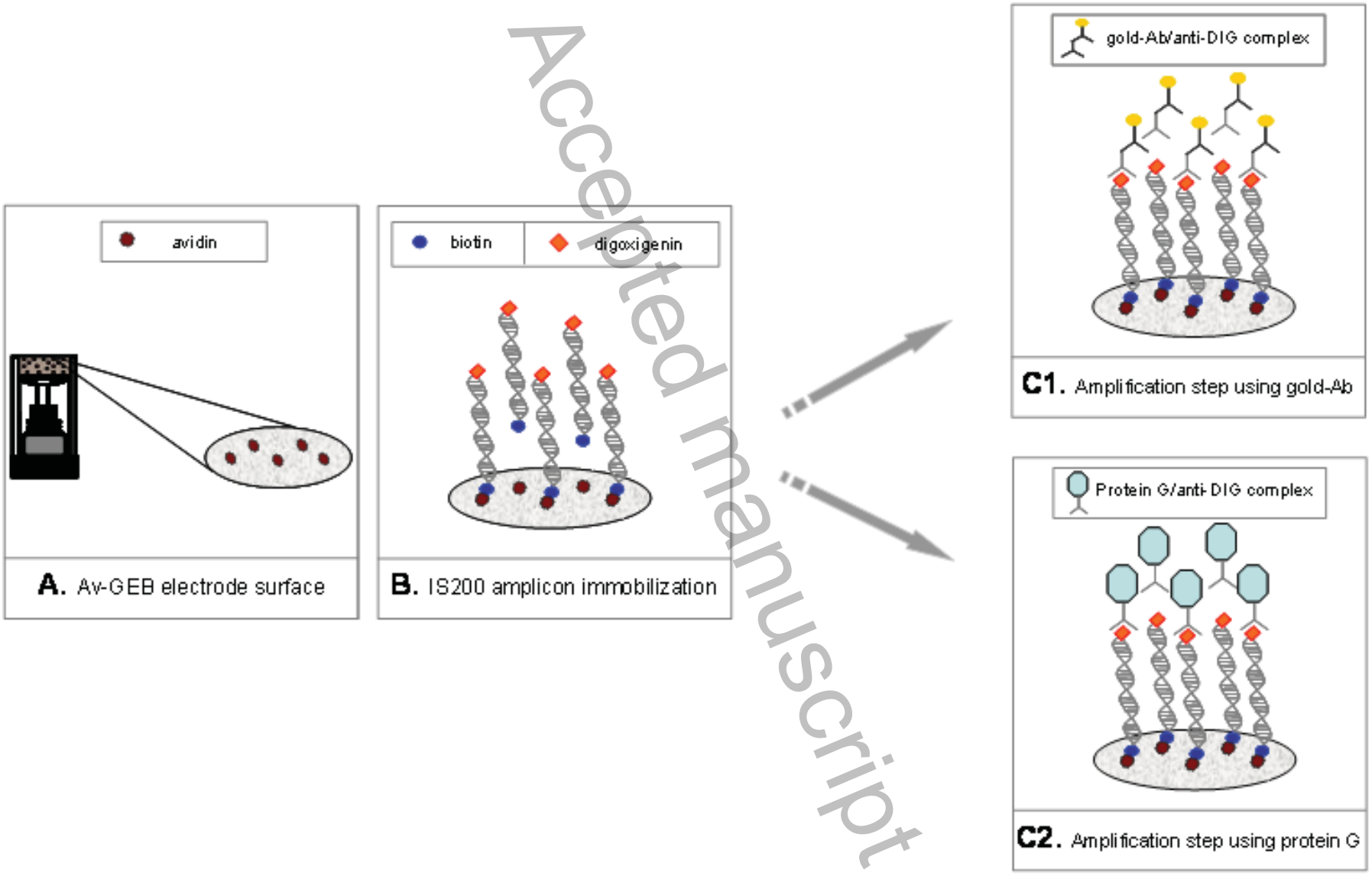

Figure 6
Click here to download Figure: FIG6.pdf

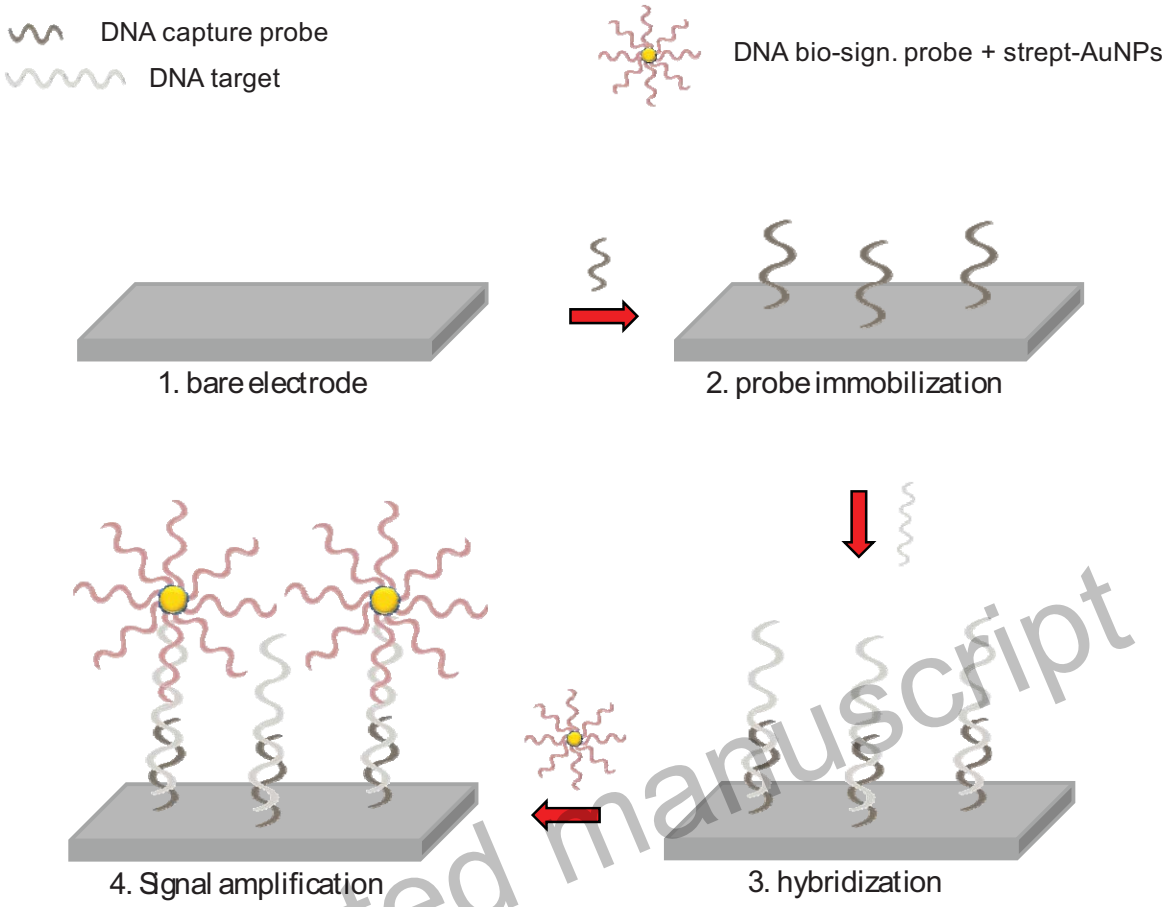

Figure 6

Figure 7

Click here to download Figure: FIG7.pdf

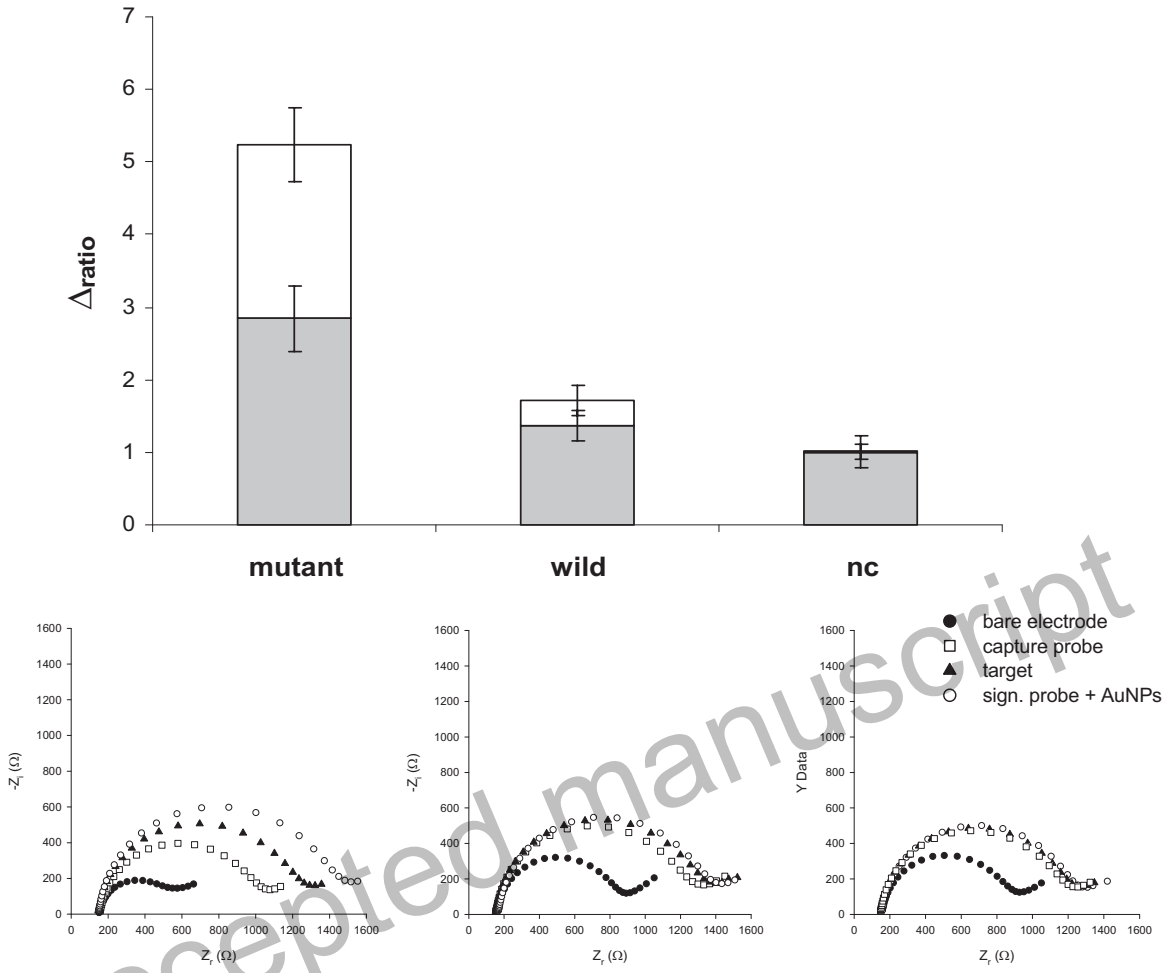

Figure 7

Figure 8
Click here to download Figure: FIG8.pdf